Water Science & Technology

IWA PUBLISHING

Water Science & Technology Vol 84 No 9, 2214 doi: 10.2166/wst.2021.437

Comparison between different infiltration models to describe the infiltration of permeable brick pavement system via a laboratory-scale experiment

Jianying Song[a], Jianlong Wang[a,b,*], Wenhai Wang[a], Liuwei Peng[b], Hongxin Li[b], Changhe Zhang[b] and Xing Fang[c]

[a] Key Laboratory of Urban Stormwater System and Water Environment (Ministry of Education), Beijing University of Civil Engineering and Architecture, Beijing, China
[b] Beijing Engineering Research Center of Sustainable Urban Sewage System Construction and Risk Control, Beijing University of Civil Engineering and Architecture, Beijing, China
[c] Department of Civil Engineering, Auburn University, Auburn, Alabama 33648, USA
*Corresponding author. E-mail: wangjianlong@bucea.edu.cn

XF, 0000-0003-4188-9013

ABSTRACT

The permeable brick pavement system (*PBPs*) is one of a widely used low impact development (*LID*) measures to alleviate runoff volume and pollution caused by urbanization. The performance of *PBPs* on decreasing runoff volume is decided by its permeability, and it was general described by hydraulic conductivity based on Darcy's law. But there is large error when using hydraulic conductivity to describe the infiltration of *PBPs*, and which infiltration process is not following Darcy's law, so it is important to find more accurate infiltration models to describe the infiltration of *PBPs*. The Horton, Philip, Green-Ampt, and Kostiakov infiltration models were selected to find an optimal model to investigate infiltration performance of *PBPs* via a laboratory-scale experiment, and the maximum absolute error (*MAE*), Bias, and coefficient of determination (R^2) were selected to evaluate the models' errors via fitting with experiment data. The results showed that the fitting accuracy of Kostiakov, Philip, and Green-Ampt models was significantly affected by the monitoring area and hydraulic gradients. Meanwhile, Horton model fitted well (*MAE* = 0.25–0.32 cm/h, Bias = 0.07–0.11 cm/h, and R^2 = 0.98–0.99) with the experiment data, and the parameters of the Horton model often can be achieved by monitoring, such as the maximum infiltration rate and the stable infiltration rate. Therefore, the Horton model is an optimal model to describe the infiltration performance of *PBPs*, which can also be adopted to evaluate hydrological characterization of *PBPs*.

Key words: Darcy's law, Green-Ampt model, Horton model, Kostiakov model, Permeable brick pavement system, Philip model

HIGHLIGHTS

- The constant and falling head monitoring methods based on Darcy's law have large error to describe the infiltration process of PBPs.
- Horton model is an optimal model used to describe the infiltration process of PBPs, and fits well with experiment data.
- Horton model is flexible under different compositions of PBPs, and the parameters of the Horton model are determined based on experiment data which can use for mointoring.

1. INTRODUCTION

Natural landscapes are being replaced by pavement with rapid urbanization, thereby increasing impervious areas and reducing permeability of landscapes (Leimgruber *et al.* 2018), this process significantly lowers the capacity to store stormwater runoff (Dong *et al.* 2019). The destruction of natural geological features and hydrological systems induces numerous ecological and environmental problems such as flooding, waterlogging, and runoff pollution (Vu & Ranzi 2017; Tam & Nga 2018). The increasing impervious urban area also increases the stormwater runoff volume and peak flow rate. Eshtawi *et al.* (2016) found that a 1% increase in impervious area would decrease the total infiltration volume from rainfall (range from 0 to −0.41 of Urban-Percolation Index) and increase the runoff volume (range from 0 to around 1 of Urban-Surface Index). Olivera & DeFee (2007) found that when the impervious area reached 10%, the annual runoff depth of the catchment increased by 146%. To alleviate these stormwater problems caused by urbanization, low impact development (*LID*)

had been proposed to reduce the runoff volume via decentralization measures at source (Hamel *et al.* 2013; Dagenais *et al.* 2017).

As one of a widely used *LID* measures with high permeability, permeable pavement (*PP*) can effectively restore the hydrological impact caused by urbanization, such as reduction of rainfall volume and peak flow, and remove runoff pollution (Sambito *et al.* 2021). The high porosity of the base layer can effectively retain stormwater runoff, recharge groundwater, and relieve the pressure on the drainage pipe network (Kamali *et al.* 2017). The function of PP is related to its infiltration performance, which is important for runoff volume reduction and pollutant removal, and *PBPs* is one type of *PP*. Most research on the infiltration performance of *PBPs* is limited on surface layer, and adopts constant head or falling head methods based on Darcy's law. Niu (2011) investigated the permeability of the surface layer of *PBPs* under different strengths and structure via constant head methods. Zhao *et al*. (2019) compared the effects of different onsite infiltration rate monitoring methods of *PBPs* and found that the double-ring method with constant head have higher accuracy when the hydraulic head was below 50 mm and the inner ring diameter was above 200 mm. Zhang (2017) derived to modify Darcy's law by equating inflow rate and infiltration rate under falling head conditions. All these studies on the infiltration performance of *PBPs* were based on Darcy's law, and limited to analysis of the surface layer, which creates a knowledge gap on the infiltration characteristics of the whole structure of *PBPs*.

Darcy (1856) designed an experiment to investigate the infiltration performance of water passing through saturated sand, and found that the infiltration volume (Q) is positive correlation with the hydraulic gradient, while the cross-sectional area (A) of the experiment column is perpendicular to the infiltration direction, and inversely proportional to the infiltration distance (L). Darcy's law is widely used to describe the infiltration characteristics of different kinds of soils, such as clay soils. Darcy's law assumes that the infiltration rate of saturated soil is linearly related to the hydraulic gradient. Hence, it is also called the linear infiltration law. In addition, many researchers have put forward different standpoints on the linear relationship of Darcy's law. Forchheimer (1901) found that the relationship between infiltration rate and hydraulic gradient gradually deviated from the linear relationship when the infiltration rate was increased. Bear (2013) summarized the limited conditions of Darcy's law, which are laminar flow and Reynolds number $<$ (1–10). More and more studies have shown that Darcy's law has limitations in describing the infiltration for some types of media. Therefore, for heterogeneous multi-layer media structures, just like *PBPs*, there needs to be further investigation to determine if Darcy's law is suitable for describing infiltration characteristics of *PBPs* or not.

Infiltration performance is important for *PBPs* to analyse its runoff volume reduction and pollutant removal. So, it is important to find an optimal infiltration model to describe the infiltration characteristics for the whole structure of *PBPs*. The objectives of this study were as follows: (1) error analysis when using Darcy's law to describe infiltration performance of *PBPs*, (2) comparing the accuracy of monitoring methods by different monitoring areas and hydraulic gradients to find optimal monitoring conditions, (3) to find an optimal model by evaluating the fitting accuracy between the experiment data and selected models under different hydraulic gradients and monitoring areas, (4) further analysis of the flexibility of the optimal model under different materials to adopt in different structure layers.

2. MATERIALS AND METHODS

2.1. Experimental device

Three experimental devices with different cross-sectional area were adopt, which was 300 × 300 mm (A_1), 400 × 400 mm (A_2), 500 × 500 mm (A_3), respectively, which was based on monitoring methods and experimental studies of PP (Chu & Fwa 2019; Zhao *et al*. 2019), the system composition of each experimental device is shown in Figure 1. Three overflow outlets with different heights were set up to keep the hydraulic head at 50, 100, and 200 mm.

The *PBPs* structure is shown in Figure 2, and the structure layers from top to bottom are surface layer (60 mm), leveling layer (40 mm), base layer (200 mm) and soil layer (100 mm). The leveling layer, base layer, and soil layer were separated by permeable geotextiles. The arrangement of permeable bricks in the surface layer is shown in Figure 3, the size of the permeable brick is 200 mm × 100 mm × 60 mm (L × W × H) and the joint width is 3 mm, which was filled with medium sand. The inside of the experimental device was glued to prevent short-cutting the infiltration pathway. The materials adopted in different layers of *PBPs* are listed in Table 1. Scheme 1 was adopted for error analysis of Darcy's law, Scheme 2 was adopted for fitting accuracy analysis of different infiltration models, and Scheme 3 was adopted for flexible analysis and parameter determination of the Horton model.

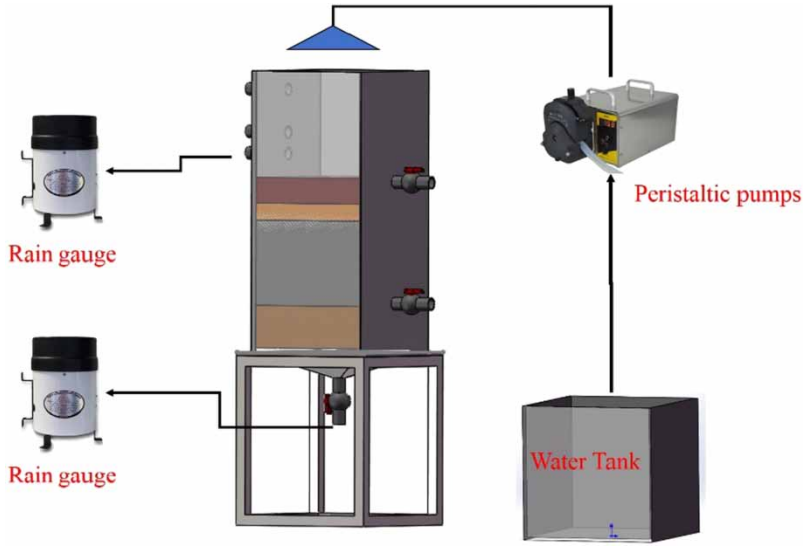

Figure 1 | Experimental process.

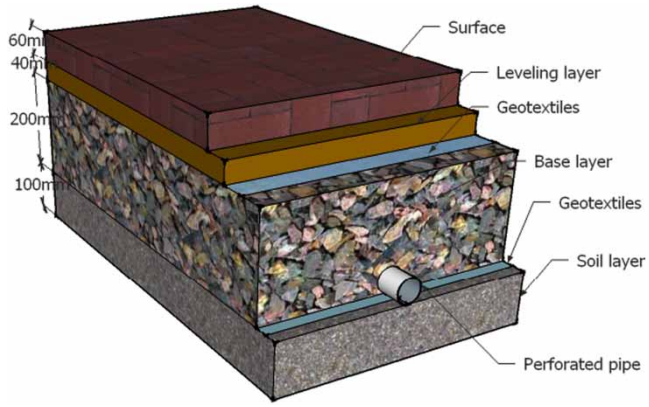

Figure 2 | The structure of *PBPs*.

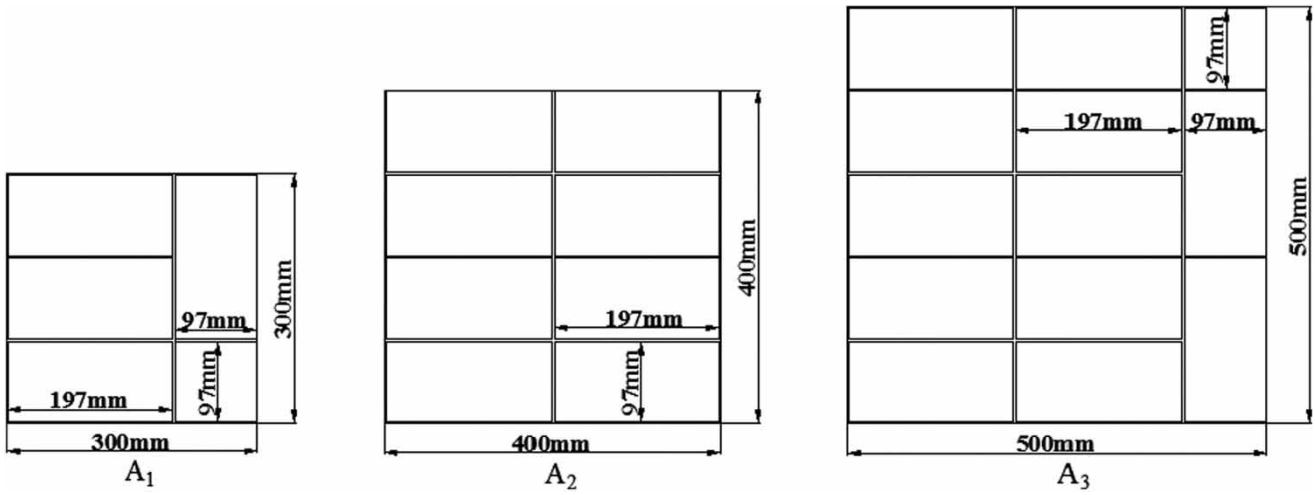

Figure 3 | The arrangement of permeable bricks in the surface layers in different experimental devices.

Table 1 | Materials in different layers

Layer types	Scheme 1	Scheme 2	Scheme 3
Surface layer	Permeable brick	Permeable brick	Permeable brick
Leveling layer	Medium sand	Medium sand	Fine, particle size: 0.25–0.35 mm Medium, particle size: 0.35–0.6 mm Coarse, particle size: 0.6–1.0 mm
Base layer	Gravel: 5–8 mm	Gravel: 5–8 mm	Gravel: 2–5 mm/5–8 mm/8–18 mm
Soil layer	Loess	Loess	Loess

2.2. Experiment methods

2.2.1. Constant and falling head methods adopted in infiltration experiments

The methods monitoring the hydraulic conductivity of *PBPs* were divided into laboratory and onsite methods. The laboratory method was used to calculate the hydraulic conductivity of the surface layer of the *PBPs* under constant hydraulic head based on Darcy's law (Equations (1) and (2)). The hydraulic conductivity of the surface layer of *PBPs* can be measured via standard test methods, such as of *EN 12697-19* (BSI 2012a) or *ASTM D2434-68* (ASTM 2006):

$$Q = k \cdot A \cdot J = k \cdot A \cdot \frac{H}{L} \tag{1}$$

$$k = \frac{QL}{AH} \tag{2}$$

where k is hydraulic conductivity, cm/s; J is hydraulic gradient, cm/cm; A is the cross-sectional area of the experiment device, cm^2; H is the hydraulic head, cm; L is the thickness of the permeable brick, cm.

The standard methods monitoring the infiltration characteristics of *PBPs* used for onsite were also limited to surface layer, which included the A*STM C1701* (ASTM 2017), *ASTM C1781* (ASTM 2015), and *NCAT* (Li Kayhanian & Harvey 2013). The infiltration rate in *ASTM C1701* and *ASTM C1781* are calculated using Equation (3) under constant head or falling head. Because the soil layer at the bottom of the *PBPs* can be considered as an infinite extension, the hydraulic gradient(J) ≈ 1, the infiltration rate is equal to the hydraulic conductivity (Equation (4)):

$$i = \frac{KM}{D^2 t} \tag{3}$$

$$Q = k \cdot A \cdot J = A \cdot i \tag{4}$$

where i is the infiltration rate, mm/h; M is the volume of infiltrated, kg; D is inner diameter of infiltration ring, mm; t is the time required for measured amount of water to infiltrate the pavement, s, K is constant value.

The *NCAT* method was developed by the National Center for Asphalt Technology in the late 1990s. The hydraulic conductivity can be calculated by Equations (5)–(7), which is also based on Darcy's law:

$$dQ = vAdt = k\frac{h}{l}Adt \tag{5}$$

$$k\frac{h}{l}Adt = -adh \tag{6}$$

$$k = \frac{al}{At}\ln\left(\frac{h_1}{h_2}\right) \tag{7}$$

where k is hydraulic conductivity, cm/s; a is the inside cross-sectional area of inlet standpipe, cm^2; t is average elapsed time of water flow between timing marks (t_1-t_2), s; h_1 is hydraulic head at time t_1, cm; h_2 is hydraulic head at time t_2, cm.

Table 2 | Experimental scheme for the different calculation methods

Case	Hydraulic head	Calculation method
Case 1	Constant head	Equation (2)
Case 2	Constant head	Equation (3)
Case 3	Falling head	Equation (3)
Case 4	Falling head	Equation (7)

All of the above calculation methods for infiltration of *PBPs* are based on Darcy's law and only limited surface layers, but there is little knowledge about which is an optimal method to describe the infiltration process for the whole structure of *PBPs*. Therefore, the errors of the different methods were investigated through laboratory-scale experiments under different conditions (Table 2).

2.2.2. Infiltration models evaluation for *PBPs*

The infiltration experiment with constant head was adopted to investigate the accuracy of four selected infiltration models. A high inflow rate was set to reach the constant head immediately at the beginning of the experiment, so that the effect of hydraulic gradient variation can be neglected. The infiltration rate was calculated based on water balance (neglecting evaporation) (Equation (8)). The constant inflow rate was maintained by peristaltic pumps (type: YZ35) during the experiment. The overflow and outflow were monitored by rain gauge (HOBORG3-M), respectively (Figure 1):

$$i = \frac{Q_{in} - Q_{over}}{A} \tag{8}$$

where i is the *PBPs* infiltration rate, cm/s; Q_{in} is the inflow rate, mL/s; and Q_{over} is the overflow rate, mL/s; A is the monitoring area, mm^2.

The infiltration rate was obtained by water balance calculation and used to evaluate the accuracy of the different infiltration models, then the flexibility of the optimal model was further analyzed by changing the material and initial moisture in different layers of the *PBPs*.

2.2.3. Calculation method of initial moisture content for *PBPs*

The effects of initial moisture content on the fitting accuracy of the different infiltration models were investigated, and the *PBPs* moisture content under the different dry periods was calculated via the weighing method (Equation (9)):

$$\beta = \frac{m_1 - m_0}{m_0} \times 100\% \tag{9}$$

where β is the moisture of the *PBPs*, %; m_1 is the wet weight of the *PBPs*, kg; m_0 is the dry weight of the *PBPs*, kg.

2.3. Introduction of infiltration models

There were several infiltration models proposed based on Darcy's law, which included Green-Ampt, Philip, Horton, Kostiakov. The Horton model was proposed in 1933 based on the infiltration of different soil types. It is a hyperosmotic-runoff model, limited to a constant head monitoring method. For its flexible parameters, the Horton model is widely used to investigate the moisture of different types of medias and used in hydraulic models to describe the infiltration performance of the pervious area (such as in *SWMM*) (Amiisi *et al.* 2020; Yang *et al.* 2020). The infiltration rate is calculated as in Equation (10):

$$i = i_c + (i_0 - i_c)\, e^{-kt} \tag{10}$$

where i is the infiltration rate, cm/min; i_c is the stable infiltration rate, cm/min; i_0 is the maximum infiltration rate, cm/min; t is infiltration time, min; k is an empirical constant.

The Kostiakov model is a widely used power function model. The relationship between infiltration rate and infiltration time of *PBPs* follows the power function, and the form of the model is similar to that of the infiltration rate curve. The infiltration

rate is calculated using Equation (11):

$$i = at^{-b} \tag{11}$$

where i is the infiltration rate, cm/min; a, b is empirical constant; and t is the infiltration time, min.

Furthermore, the Philip model (Philip 1957) is based on unsaturated semi-infinite soil vertical infiltration conditions and the Richards equation. The model describes the one-dimensional vertical infiltration performance of the soil, and the constant hydraulic head ensures that the initial infiltration is one-dimensional. The model is simple and with a high accuracy in describing the soil infiltration process (Haghighi *et al.* 2010; Zolfaghari *et al.* 2012). The infiltration rate can be calculated via Equation (12):

$$i = \frac{1}{2}St^{-1/2} + A \tag{12}$$

where i is the infiltration rate, cm/min; S is the moisture absorption rate, cm/min, indicating the capacity of soil water absorption caused by the matrix potential difference; and A is the steady infiltration rate, cm/min. The A value is equal to the steady infiltration rate i_c in the Horton model when the infiltration time is long enough.

The Green-Ampt model is a physical model of soil infiltration, which was proposed by Green and Ampt in 1911 based on capillary theory. Green-Ampt assumed that there exists a wetting front in the water-bearing soil profile during the infiltration process, and that the soil moisture content is saturated between the wetting front and the soil surface, whereas a constant suction force exists at the wetting front. The infiltration rate can be calculated via Equation (13):

$$i = k_s \frac{Z_f + S_f + H}{Z_f} \tag{13}$$

where i is the soil infiltration rate, cm/min; k_s is the saturated hydraulic conductivity, cm/min; H is the water depth above soil surface, cm; S_f is the wetting front suction, cm; Z_f is the wetting front depth, cm.

2.4. Evaluation methods for comparing the errors between different infiltration models and experimental data

Several evaluation methods were selected to evaluate the fitting accuracy between the different infiltration models and experimental data. The coefficient of determination (R^2) in Equation (14) is an indicator that evaluates the fitting accuracy (Al-Safi & Sarukkalige 2020):

$$R^2 = \frac{\left[\sum_{i=1}^{n}(y_i - \bar{y})(\hat{y}_i - \overline{\hat{y}_i})\right]^2}{\sum_{i=1}^{n}(y_i - \bar{y})^2 \sum_{i=1}^{n}(\hat{y}_i - \overline{\hat{y}_i})^2} \tag{14}$$

where R^2 is the coefficient of determination (between 0 and 1); $\hat{y}_i$ is the fitted value; y_i is the observed value; $\bar{y}$ is the observed mean value; $\overline{\hat{y}_i}$ is the mean fitted value.

The maximum absolute error (*MAE*) was used to evaluate the maximum error between the fitted value of different models and the experiment data. The *MAE* can be calculated using following equation:

$$MAE = \max(|y_i - \hat{y}_i|) \tag{15}$$

The bias was used to evaluate the average difference between the fitted value of the infiltration models and the experiment data. It reflects the deviation of the fitted value from the observed value, which can be calculating using following equation:

$$\text{Bias} = \frac{\sum_{i=1}^{n}(|y_i - \hat{y}_i|)}{n} \tag{16}$$

3. RESULTS AND DISCUSSION

3.1. Error analysis of Darcy's law to describe infiltration performance of the whole structure of *PBPs*

The hydraulic conductivity of the whole structure of *PBPs* under various monitoring areas and hydraulic gradients were calculated by constant and falling head methods, respectively, according Equations (2), (3), and (7). The maximum infiltration rate (i_0), steady infiltration rate (i_c), and hydraulic conductivity for Case 1 are shown in Figure 4. The hydraulic conductivity was the smallest among the hydraulic conductivities, i_0, and i_c, they all increased as the hydraulic gradient increased. When the monitoring area was A_1, i_0 had the largest error with the hydraulic conductivity calculated by Darcy's law, and the deviation was 20.62, 18.21, and 15.80 cm/h when the hydraulic head was 50, 100, and 200 mm, respectively. The error between the i_0 and the hydraulic conductivity decreased as the monitoring area increased. The deviation varied between 8.84 and 9.31 cm/h when the monitoring area was A_3. The error between the i_c and hydraulic conductivity at different monitoring areas and hydraulic gradients also showed a large deviation of 1.42–7.27 cm/h. Further analysis was processed to find the relationship between hydraulic conductivity and hydraulic gradients, and the hydraulic conductivity ranged between 7.91 and 14.33 cm/h when the monitoring area was A_1. In addition, Darcy's law assumption is that there is a linear relationship between the infiltration rate and the hydraulic gradient, and that the hydraulic conductivity would remain constant under different hydraulic gradients. Therefore, there exists large errors when using Darcy's law to describe the infiltration performance for the whole structure of *PBPs*, whatever the saturation.

The maximum infiltration rate (i_0), steady infiltration rate (i_c), and the hydraulic conductivity calculated by different onsite monitoring methods are shown in Figure 5. The deviation between i_0 and hydraulic conductivity is large under different hydraulic gradients, and the range is 6.15–19.03 cm/h, especially when the monitoring area was A_1, and the hydraulic

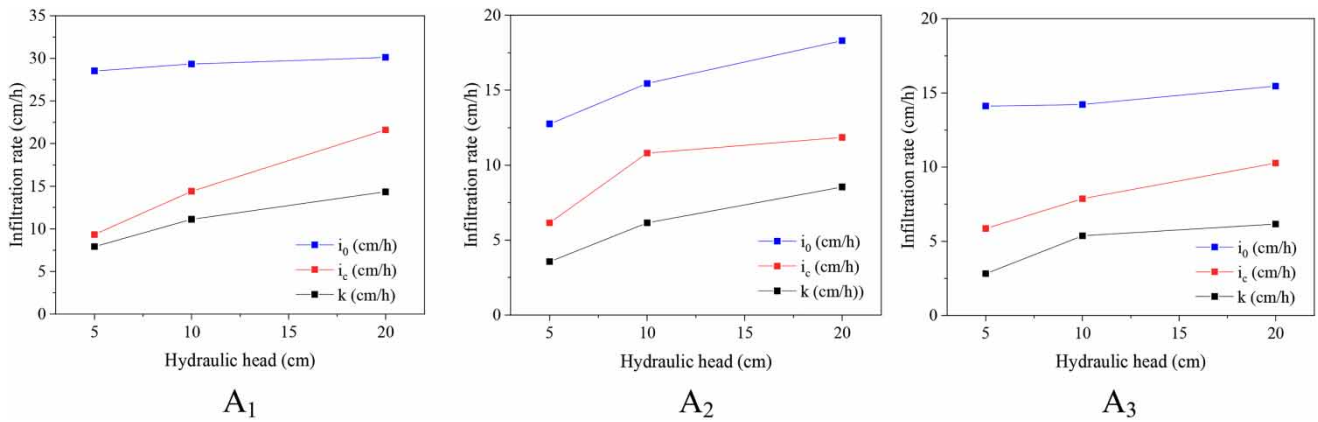

Figure 4 | Error analysis of Darcy's law with Case 1.

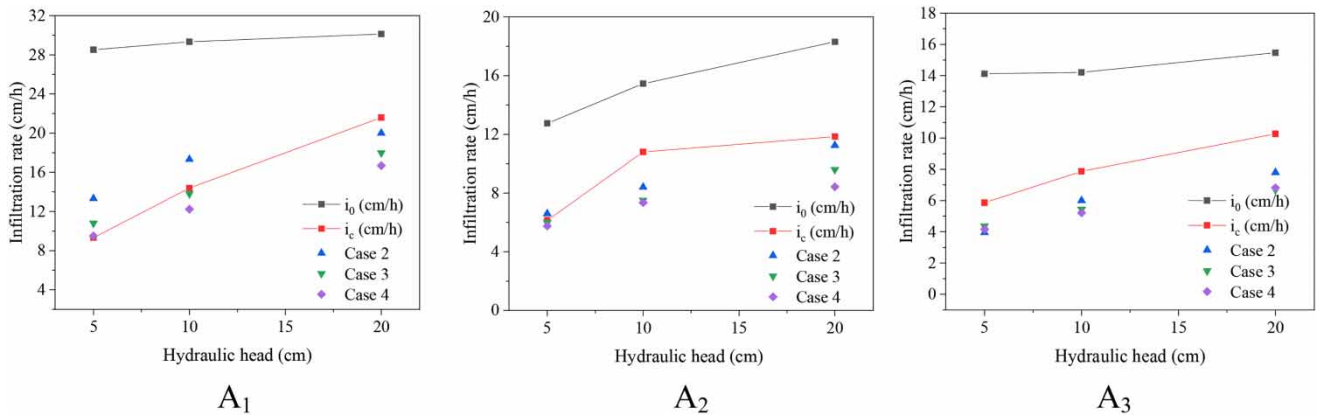

Figure 5 | Error analysis of different onsite monitoring methods.

head was 50 mm. The deviation between i_0 and the hydraulic conductivity calculated by Cases 2, 3, and 4 were 15.20, 17.73, and 19.03 cm/h, respectively. Whereas, there was minimum deviation between i_0 and hydraulic conductivity (6.15, 6.75, and 7.00 cm/h) when the monitoring area was A_2, and the hydraulic head was 50 mm. The error between i_c and hydraulic conductivity was minimum (calculated by three *in situ* monitoring calculation methods) when the hydraulic head was 50 mm and the monitoring area was A_2. The deviation between i_c and the hydraulic conductivity calculated by Cases 2, 3, and 4 was 0.45, 0.15, and 0.40 cm/h, respectively. Whereas, the maximum deviation was 4.91 cm/h when the area was A_1. So, the error of hydraulic conductivity by monitoring is affect by hydraulic head and monitoring area.

Through error analysis of different monitoring methods, the results showed that the different monitoring methods used for infiltration rate calculation of *PBPs* all have errors. Specifically, the hydraulic conductivity calculated by Darcy's law with constant head had maximum error (Case 1). The error between the hydraulic conductivity and the experimental infiltration rate decreased gradually with the monitoring area increased. The infiltration rate had a lower error than hydraulic conductivity, especially when the hydraulic head was 50 mm and the monitoring area was A_2, the deviation between i_c and Cases 1, 2, 3, and 4 was 2.59, 0.45, 0.15, and 0.40, respectively. Therefore, the optimal monitoring area and hydraulic gradient need to be selected to reduce the monitoring errors.

The applicable conditions of Darcy's law from theoretical analysis including: (1) temperature kept constant during the whole infiltration process, (2) infiltration flow kept laminar flow during the whole infiltration process, (3) porous medium is homogeneous and isotropic, and (4) infiltration rate and hydraulic gradient conforming to a linear relationship (Zhang *et al.* 2018), which is different with infiltration of *PBPs*. The surface layer of *PBPs* is non-homogeneous and consists of brick and brick joints. Brick is a porous media, while the brick joints are filled with sand (Chu & Fwa 2019). In addition, the *PBPs* is a multi-layer and non-homogeneous media, with different porosity and density at each layer, which results in the inertia force and viscous force of infiltration in each layer being different, so the infiltration rate in each layer is different, the relationship between the infiltration rate and hydraulic gradient was nonlinear. So, all of these differences may be the main reason that caused the large errors when using Darcy's law to describe the infiltration performance for whole structure of *PBPs*.

3.2. Comparing the fitting accuracy between experimental data and different infiltration models

The fitting results of the selected infiltration models under different monitoring areas and hydraulic gradients are shown in Tables 3–5 (*H* is Horton model; *P* is Philip model; *G* is Green-Ampt model and *K* is Kostiakov model). The Horton model fitted well under the different monitoring areas, with R^2 values of 0.98–0.99, 0.98–0.99, and 0.97–0.99 for A_1, A_2, and A_3, respectively. The average values of *MAE* were 1.04, 0.29, and 0.37 cm/h, while the biases were 0.30, 0.09, and 0.12 cm/h, respectively. When the hydraulic head was 100 mm, the Horton model fitted better with R^2 of 0.98–0.99, the minimum

Table 3 | Fitting results of different infiltration models with monitoring area of A_1

	R^2			Bias (cm/h)			MAE (cm/h)		
Model	H = 50 mm	H = 100 mm	H = 200 mm	H = 50 mm	H = 100 mm	H = 200 mm	H = 50 mm	H = 100 mm	H = 200 mm
H	0.98	0.98	0.99	0.40	0.38	0.11	1.34	1.40	0.39
P	0.95	0.98	0.98	0.74	0.42	0.51	3.51	1.31	1.62
G	0.99	0.99	0.99	1.03	0.59	0.34	2.53	1.48	0.73
K	0.95	0.99	0.93	0.84	0.16	0.26	3.19	0.56	0.70

Table 4 | Fitting results of different infiltration models with monitoring area of A_2

	R^2			Bias (cm/h)			MAE (cm/h)		
Model	H = 50 mm	H = 100 mm	H = 200 mm	H = 50 mm	H = 100 mm	H = 200 mm	H = 50 mm	H = 100 mm	H = 200 mm
H	0.99	0.98	0.99	0.07	0.11	0.08	0.25	0.31	0.32
P	0.92	0.96	0.90	0.42	0.18	0.29	1.50	0.67	1.42
G	0.99	0.99	0.99	0.31	0.17	0.09	0.72	0.66	0.31
K	0.96	0.98	0.97	0.26	0.12	0.25	0.97	0.42	0.81

Table 5 | Fitting results of different infiltration models with monitoring area of A_3

	R^2			Bias (cm/h)			MAE (cm/h)		
Model	H = 50 mm	H = 100 mm	H = 200 mm	H = 50 mm	H = 100 mm	H = 200 mm	H = 50 mm	H = 100 mm	H = 200 mm
H	0.97	0.99	0.98	0.16	0.07	0.12	0.39	0.25	0.47
P	0.74	0.84	0.89	1.07	0.57	0.4	4.29	2.27	1.37
G	0.99	0.99	0.99	0.21	0.17	0.18	0.39	0.42	0.37
K	0.85	0.94	0.95	0.90	0.33	0.25	3.19	1.44	0.81

MAE was 0.25–0.32 cm/h, and the bias was 0.07–0.11 cm/h. Thus, the Horton model fitted better than other models under different experiment conditions.

The fitting accuracy of Philip model varied significantly among the different monitoring areas, R^2 was ranged between 0.74 and 0.98, *MAE* was ranged between 0.67 and 4.29 cm/h and bias was ranged between 0.18 and 1.07 cm/h. The Philip model had poor fitting accuracy ($R^2 = 0.74$, bias = 1.07 cm/h, and $MAE = 4.29$ cm/h) when the monitoring areas was A_3 and hydraulic head was 50 mm. Therefore, the Philip model had large errors when describing the infiltration process of *PBPs*, especially in large monitoring areas. The R^2 of the Kostiakov model was ranged between 0.93–0.99, 0.96–0.98, and 0.85–0.95, when monitoring areas were A_1, A_2, and A_3, respectively, but the fitting accuracy of which is significantly lower at low hydraulic gradients. The R^2, bias and *MAE* were 0.85, 0.90 cm/h, and 3.19 cm/h respectively, when the monitoring area was A_3 and hydraulic head was 50 mm. Therefore the accuracy of Philip and Kostiakov models was lower than the Horton model, and the fitting accuracy was significantly affected by monitoring area and hydraulic head.

The Horton, Philip and Kostiakov models fitted well with experiment data when the monitoring area was A_2 (Tables 3–5). The fitting accuracy of different models was further analysed by profiles of infiltration rate changing with time elapse (Figure 6). The infiltration rate decreased gradually with the infiltration time elapse, the i_0 and i_c increased when the hydraulic gradient was increased, while stable infiltration time changed little under different hydraulic gradients which and ranged from 300 to 345s. The Philip and Kostiakov models showed large deviations at the beginning and stabilization stages of the whole infiltration process, the range of deviation in the beginning stages was 0.58–1.50 cm/h and 0.03–0.97 cm/h, whereas the Horton model was fitted well into the whole infiltration process of *PBPs*.

The Green-Ampt model (Figure 7) describes by the relationship of cumulative infiltration volume and infiltration continuous time, which fitted well with the experimental data. The cumulative infiltration volume and infiltration continuous time followed a linear relationship with different monitoring areas. Thus, the variation range of infiltration rate decreased when the monitoring area was increased. The infiltration rate had a minimal variation range (10.27–15.46 cm/h) when the monitoring area was A_3 and hydraulic head was 200 mm. Furthermore, a polynomial was used to convert the cumulative infiltration volume into infiltration rate. It can be found that the fitting accuracy of the Green-Ampt model was increased with the monitoring area and hydraulic gradient increasing by comparing Tables 3–5. The Horton model fitted well under the different hydraulic gradients when the monitoring area was A_3, and the bias was 0.21, 0.17, and 0.18 cm/h, when hydraulic gradient was 50, 100, and 200 mm, respectively.

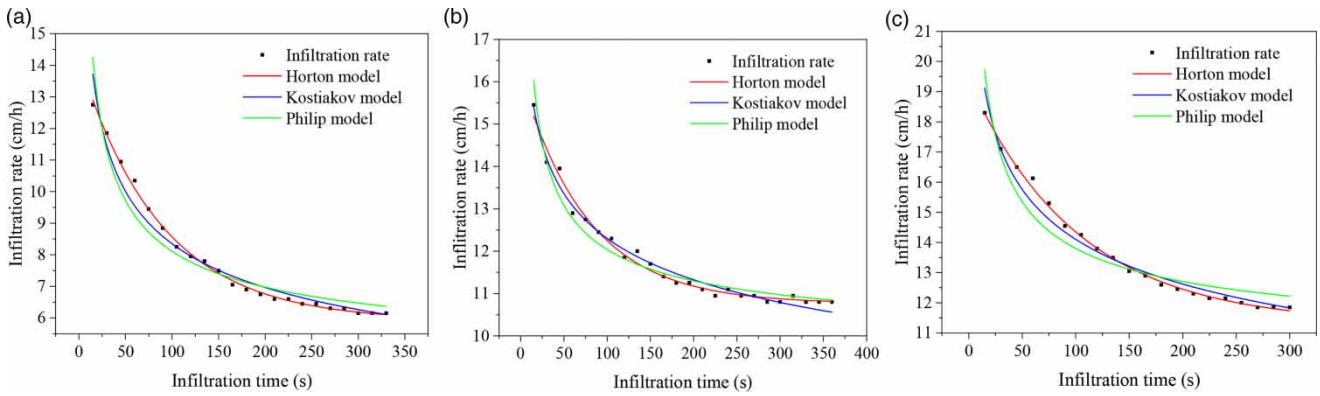

Figure 6 | Infiltration rates with different hydraulic gradients ((a) 50 mm, (b) 100 mm, (c) 200 mm).

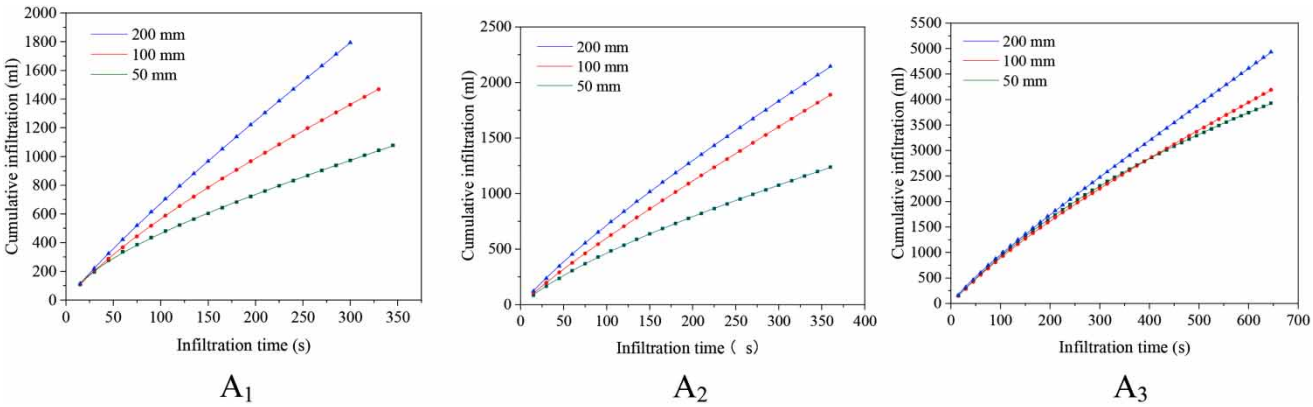

Figure 7 | The fitting results of Green-Ampt model under different monitoring areas and hydraulic gradients.

Therefore, the Horton model fitted well to describe the infiltration performance for the whole structure of the *PBPs*, which was little affected by monitoring area and hydraulic gradient. Meanwhile, the fitting accuracy of Kostiakov, Philip, and Green-Ampt models was affected greatly by the monitoring area and hydraulic gradient. The MAE, bias, R^2, advantage and disadvantage of different infiltration of different models are listed in Table 6. Though comparison of data in Table 6, it can be found that the fitting accuracy of different infiltration models followed the sequence Horton > Green-Ampt > Kostiakov > Philip.

The parameters of the Horton model had physical meaning, therefore, the fitting accuracy was further analyzed based on the errors between the fitting values and the experiment data (i_0 and i_c), as shown in Figure 8, i_c and $i_0 - i_c$ fitted well with the experimental data when the hydraulic head was 100 mm, the errors of i_c were 1.15%, 0.34%, 5.28%, while the $i_0 - i_c$ were 12.94%, 15.39%, 15.56%, when the monitoring area was A_1, A_2, and A_3, respectively. When the monitoring area was A_2 and the hydraulic head was 100 mm, the Horton model had the maximum R^2, the minimum bias and *MAE*, and had a high fitting accuracy between the fitted parameters and the experimental data. So, the Horton model is an optimal model that can be used to describe the infiltration performance for the whole structure of *PBPs*, but the fitting accuracy and flexible of Horton model need to be further analyzed to improve the accuracy in advance.

3.3. Flexible analysis and parameters determination of Horton model

The flexibility of the Horton model was further analyzed, and its parameters were determined by changing the materials in different layers and initial moisture content when the monitoring area was A_2 and the hydraulic head was 100 mm. The

Table 6 | Comparison of different infiltration models for describing infiltration performance of *PBPs*

	MAE (cm/h)		Bias (cm/h)		R^2			
Infiltration models	**Variation range**	**Average value**	**Variation range**	**Average value**	**Variation range**	**Average value**	**Advantages**	**Disadvantages**
Horton	0.25–1.40	0.57	0.07–0.40	0.17	0.97–0.99	0.98	The model is flexible and have high fitting accuracy under different infiltration conditions.	The particle size of the material used in the leveling layer greatly affected the accuracy.
Green-Ampt	0.31–2.53	0.84	0.09–1.03	0.34	0.99–0.99	0.99	The model fitted well when the hydraulic head is high and in large monitoring areas.	The model has large error when the monitoring area and hydraulic gradient were small.
Kostiakov	0.42–3.19	1.34	0.12–0.90	0.37	0.85–0.99	0.95	The model was fitting well when the hydraulic head is high.	The fitting accuracy is poor at low hydraulic gradients.
Philip	0.67–4.29	2.00	0.18–1.07	0.51	0.74–0.98	0.90	The model has only two parameters and they were all easy to determine.	The model has poor accuracy under any monitoring condition.

accuracy under the different materials was adopted in the leveling layer and base layer, and the effect of different initial moisture content which is shown in Figure 9. When the leveling layer was filled with fine sand, medium sand, or coarse sand, the stable infiltration rates were 7.95, 10.80, and 12.75 cm/h, respectively. Moreover, the stable infiltration rates ranged from 9.75 to 11.25 cm/h under different gravel sizes of the base layer. So, the infiltration rate of the *PBPs* was significantly impacted by material particle size of the leveling layer, while the gravel size of base layer was affected slightly. The effect of initial moisture content on the stable infiltration rate can be almost neglected, and the value of stable infiltration rate was all approximately equal to 10.8 cm/h.

The errors of the Horton model under different materials and initial moisture contents are shown in Table 7, in which R^2, bias, *MAE* was 0.98, 0.05–0.14 cm/h, 0.12–0.51 cm/h, respectively. The results showed that the Horton model fitted well to describe the infiltration process of *PBPs* under different conditions, especially when the material of the leveling layer was fine sand.

The accuracy of the Horton model was further analyzed based on the errors between the fitted parameters and experimental data (Figure 10). The error of i_c was <1.60%, the $i_0 - i_c$ was <20%, except for the i_c and $i_0 - i_c$ errors which were 4.20% and 29.4%, respectively, when the material of leveling layer was coarse sand. Because of the large particle size of coarse sand, this leads to an increase in infiltration rate of *PBPs*, which affects the fitting accuracy of the model. The fitted parameters are listed in Table 8. It can be found that the k value varied within 0.012–0.013, but decreased to 0.010 when the leveling layer was coarse sand. So, the error should also be considered when using Horton model to describe infiltration performance of *PBPs* when the material of leveling layer was coarse sand.

The i_0 and i_c drawn from the experimental data were adopted in the Horton model, and the errors are shown in Table 9. It can be found that the Horton model is flexible, and kept good accuracy under different gravel sizes of the base layer and initial

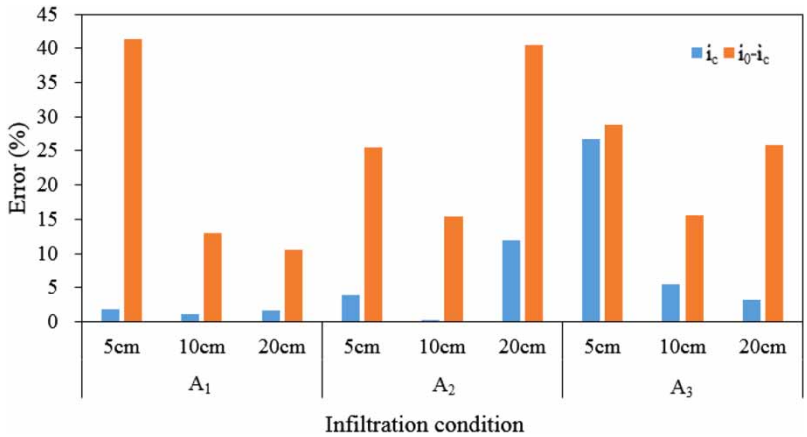

Figure 8 | Error analysis of the Horton model under different experiment conditions.

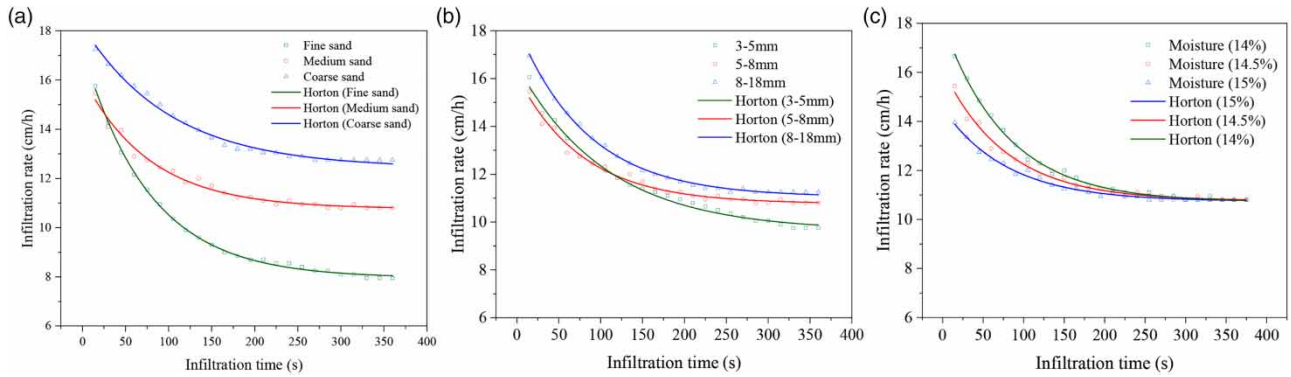

Figure 9 | Fitting results of the Horton model under the different materials and initial moisture contents ((a) Leveling layer, (b) Base layer, (c) Initial moisture contents).

Table 7 | Errors of the Horton model under different materials and initial moisture contents

Experimental conditions	MAE (cm/h)	Bias (cm/h)	R^2
Gravel			
3–5 mm	0.41	0.14	0.99
5–8 mm	0.31	0.11	0.98
8–18 mm	0.13	0.05	0.99
Initial moisture content			
14%	0.12	0.07	0.99
14.5%	0.31	0.11	0.98
15%	0.51	0.10	0.99
Sand			
Fine	0.17	0.07	0.99
Medium	0.31	0.11	0.98
Coarse	0.22	0.09	0.99

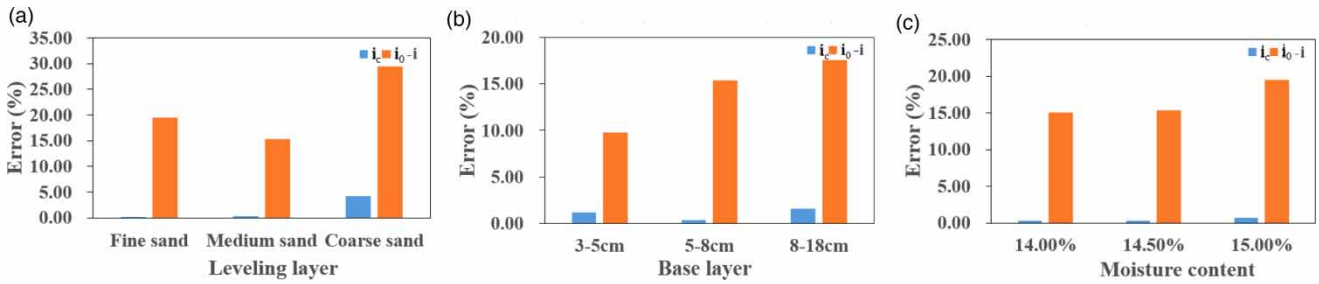

Figure 10 | Error analysis of the Horton model parameters under different infiltration conditions ((a) Leveling layer, (b) Base layer, (c) Moisture content).

moisture contents. The R^2 were all more than 0.96, and the biases were 0.12–0.18 cm/h and 0.12–0.14 cm/h, respectively. The accuracy of the Horton model decreased slightly with increasing initial moisture and gravel size. The Horton model's accuracy reduced significantly when the leveling layer was filled with coarse sand, and the R^2 was 0.95, the bias was 0.31 cm/h. This may

Table 8 | Parameters of the Horton model under different conditions

Experimental conditions	i_c (cm/min)	i_0-i_c (cm/min)	k
Gravel			
3–5 mm	9.63	6.92	0.012
5–8 mm	10.76	5.37	0.013
8–18 mm	10.97	6.70	0.012
Initial moisture content			
14%	10.77	7.19	0.013
14.5%	10.76	5.37	0.013
15%	10.73	3.79	0.012
Sand			
Fine	7.95	9.32	0.013
Medium	10.76	5.37	0.013
Coarse	12.21	5.89	0.010

Table 9 | Errors of the Horton model in advance analysis

Experimental conditions	MAE (cm/h)	Bias (cm/h)	R^2
Base layer			
3–5 mm	0.80	0.15	0.98
5–8 mm	0.74	0.12	0.97
8–18 mm	0.91	0.18	0.98
Initial moisture content			
14%	0.39	0.13	0.98
14.5%	0.74	0.12	0.97
15%	0.79	0.14	0.96
Leveling layer			
Fine	0.61	0.17	0.98
Medium	0.74	0.12	0.97
Coarse	0.56	0.31	0.95

Note: i_0 and i_c were drawn from experimental data.

be attributed to a significant increase in the infiltration rate. The k value of the model was also varied at 0.012–0.013 when the parameters were adopted from experimental data, but which was decreased to 0.010 when the leveling layer was coarse sand. Therefore, the Horton model is flexible and had higher accuracy compared with other infiltration models, for which parameters can be determined via onsite monitoring especially when the material particle size of the leveling layer is small.

4. CONCLUSION

Permeable brick pavement system (*PBPs*) is a multi-layered media structure, whose infiltration performance is critical for evaluation of runoff volume reduction and pollutant removal. The following conclusions can be drawn from the results of this study.

The experimental results showed that Darcy's law has limitation in describing the infiltration performance for whole structure of *PBPs*, and the accuracy of monitoring methods was greatly affected by monitoring area and hydraulic gradient. The constant and falling head methods all produced large errors for infiltration performance monitoring of *PBPs*, especially the laboratory monitoring method (Case1) had larger errors to describe the infiltration process of *PBPs*.

The Horton model was the optimal model when comparing the errors between Horton, Philip, Green-Ampt, and Kostiakov infiltration models and experimental data, for which R^2 ranged between 0.98 and 0.99, bias ranged between 0.07 and 0.11 cm/h, and *MAE* ranged between 0.25 and 0.32 cm/h. The accuracy of Philip, Green-Ampt, and Kostiakov infiltration models was markedly affected by monitoring area and hydraulic gradient, and produced large errors for describing infiltration performance of *PBPs*.

Although the Horton model fitted well for *PBPs* infiltration calculation, the fitting accuracy reduced when the leveling layer filled with large particle size material. The Horton model is flexible when the monitoring area was 400 mm × 400 mm and hydraulic head was 100 mm, and can be used to describe infiltration performance for the whole structure of *PBPs*, especially for the onsite monitoring method under constant head conditions, and to evaluate the effect of rainwater runoff alleviation. The Horton model is an optimal and flexible infiltration model that can be used as a monitoring and calculation method of *PBPs* infiltration, and can be adopted for hydrological evaluation and parameters to determine the infiltration model of *PBPs*.

ACKNOWLEDGEMENTS

We gratefully acknowledge the support of the National Water Pollution Control and Management Technology Major Project (No. 2017ZX07103-002), and International Science Editing for editing this manuscript.

CONFLICTS OF INTEREST

The authors declare no conflicts of interest.

DATA AVAILABILITY STATEMENT

All relevant data are included in the paper or its Supplementary Information.

REFERENCES

Al-Safi, H. I. J. & Sarukkalige, P. R. 2020 The application of conceptual modelling to assess the impacts of future climate change on the hydrological response of the Harvey River catchment. *Journal of Hydro-Environment Research* **28**, 22–33.

Amiisi, L., Wambua, R. M. & Kundu, P. M. 2020 Prediction of infiltration rate in different land use types using modified Horton equations in Upper Njoro River Catchment. In: *13th International Conference*.

ASTM, 2006. ASTM D2434-68 – Standard Test Method for Permeability of Granular Soils (Constant Head). ASTM International, West Conshohocken, PA 2006.

ASTM, 2015. ASTM C1781/C1781M – 15 Standard Test Method for Surface Infiltration Rate of Permeable Unit Pavement Systems. ASTM International, West Conshohocken, PA.

ASTM, 2017. ASTM C1701/C1701M-17a – Standard Test Method for Infiltration Rate of in Place Pervious Concrete. ASTM International, West Conshohocken, PA.

Bear, J. 2013 *Dynamics of Fluids in Porous Media*. Courier Corporation.

BSI, 2012a. Bituminous Mixtures – Test Methods for Hot Mix Asphalt Part 19: Permeability of Specimen. British Standards Institute, London, UK.

Chu, L. & Fwa, T. F. 2019 Evaluation of surface infiltration performance of permeable pavements. *Journal of Environmental Management* **238**, 136–143.

Dagenais, D., Thomas, I. & Paquette, S. 2017 Siting Green stormwater infrastructure in a neighbourhood to maximise secondary benefits: lessons learned from a pilot project. *Landscape Research* **42**, 195–210.

Darcy, H. P. G. 1856 *Les Fontaines publiques de la ville de Dijon. Exposition et application des principes à suivre et des formules à employer dans les questions de distribution d'eau, etc.* (V. Dalamont).

Dong, R., Zhang, X. & Li, H. 2019 Constructing the ecological security pattern for sponge city: a case study in Zhengzhou, China. *Water* **11**, 284.

Eshtawi, T., Evers, M. & Tischbein, B. 2016 Quantifying the impact of urban area expansion on groundwater recharge and surface runoff. *Hydrological Sciences Journal* **61**, 826–843.

Forchheimer, P. 1901 Wasserbewegung durch boden. Zeitschrift Des Vereines Deutscher Ingenieure **45**, 1782–1788.

Haghighi, F., Gorji, M., Shorafa, M., Sarmadian, F. & Mohammadi, M. H. 2010 Evaluation of some infiltration models and hydraulic parameters. *Spanish Journal of Agricultural Research* **8**, 210–217.

Hamel, P., Daly, E. & Fletcher, T. D. 2013 Source-control stormwater management for mitigating the impacts of urbanisation on baseflow: a review. *Journal of Hydrology* **485**, 201–211.

Kamali, M., Delkash, M. & Tajrishy, M. 2017 Evaluation of permeable pavement responses to urban surface runoff. *Journal of Environmental Management* **187**, 43–53.

Leimgruber, J., Krebs, G., Camhy, D. & Muschalla, D. 2018 Sensitivity of model-based water balance to low impact development parameters. *Water* **10**, 1838.

Li, H., Kayhanian, M. & Harvey, J. T. 2013 Comparative field permeability measurement of permeable pavements using ASTM c1701 and NCAT permeameter methods. *Journal of Environmental Management* **118**, 144–152.

Niu, C. 2011 *A Study on Characteristics and Design Development of Permeable Sidewalk Structure*.

Olivera, F. & DeFee, B. B. 2007 Urbanization and Its effect on runoff in the Whiteoak Bayou Watershed, Texas 1. *Journal of the American Water Resources Association* **43**, 170–182.

Philip, J. R. 1957 The theory of infiltration: 4. Sorptivity and algebraic infiltration equations. *Soil Science* **84**, 257–264.

Sambito, M., Severino, A., Freni, G. & Neduzha, L. 2021 A systematic review of the hydrological, environmental and durability performance of permeable pavement systems. *Sustainability* **13**, 4509.

Tam, V. T. & Nga, T. T. V. 2018 Assessment of urbanization impact on groundwater resources in Hanoi, Vietnam. *Journal of Environmental Management* **227**, 107–116.

Vu, T. T. & Ranzi, R. 2017 Flood risk assessment and coping capacity of floods in central Vietnam. *Journal of Hydro-Environment Research* **14**, 44–60.

Yang, M., Zhang, Y. & Pan, X. 2020 Improving the Horton infiltration equation by considering soil moisture variation. *Journal of Hydrology* **586**, 124864.

Zhang, X., Zhang, X., Taira, H. & Liu, H. 2018 Error of Darcy's law for serpentine flow fields: an analytical approach. *International Journal of Hydrogen Energy* **43**, 6686–6695.

Zhang, J. 2017 A permeability coefficient tester for permeable pavement. China Patent No. 201721815331.6.

Zhao, J., Yaqian, Z., Xi, X., Chentong, L., Zhen, W. & Haoran, J. 2019 Comparison of field permeability test methods for permeable pavement. *China Water & Wastewater* **5**, 28.

Zolfaghari, A. A., Mirzaee, S. & Gorji, M. 2012 Comparison of different models for estimating cumulative infiltration. *International Journal of Soil Science* **7**, 108–115.

First received 25 July 2021; accepted in revised form 21 September 2021. Available online 4 October 2021